Time-Resolved X-Ray Emission Spectroscopy and Synthetic High Spin Model Complexes Resolve Ambiguities in Excited State Assignments of Transition Metal Chromophores: A Case Study of Fe-Amido Complexes

Marco E. Reinhard,[a†] Baldeep K. Sidhu[b†] Issiah B. Lozada,[b†] Natalia Powers-Riggs,[c†] Robert J. Ortiz,[b] Hyeongtaek Lim[c] Rachel Nickel,[d] Johan van Lierop,[d] Roberto Alonso-Mori,[e] Matthieu Chollet,[e] Leland B. Gee,[e] Patrick L. Kramer,[e] Thomas Kroll,[a] Sumana L. Raj,[e] Tim B. van Driel,[e] Amy A. Cordones,[c] Dimosthenis Sokaras,[a] David E. Herbert[b]* and Kelly J. Gaffney[c]**

[a] Stanford Synchrotron Radiation Lightsource, SLAC National Accelerator Laboratory, 2575 Sand Hill Road, Menlo Park, CA 94025, USA; *dsokaras@slac.stanford.edu

[b] Department of Chemistry and the Manitoba Institute for Materials, University of Manitoba, 144 Dysart Rd, Winnipeg, MB, R3T 2N2, Canada; *david.herbert@umanitoba.ca

[c] Stanford PULSE Institute, SLAC National Accelerator Laboratory, 2575 Sand Hill Road, Menlo Park, CA 94025, USA; *kgaffney@slac.stanford.edu

[d] Department of Physics and Astronomy, University of Manitoba, 31A Sifton Rd, Winnipeg, MB, R3T 2N2, Canada

[e] Linac Coherent Light Source, SLAC National Accelerator Laboratory, 2575 Sand Hill Road, Menlo Park, CA 94025, USA

[†] These authors contributed equally to this work.

ABSTRACT

To fully harness the potential of abundant metal coordination complex photosensitizers, a detailed understanding of the molecular properties that dictate and control the electronic excited state population dynamics initiated by light absorption is critical. In the absence of detectable luminescence, optical transient absorption (TA) spectroscopy is the most widely employed method for interpreting the electron redistribution in such excited states, particularly for those with charge-transfer character. The assignment of excited state TA spectral features often relies on spectroelectrochemical measurements, where the transient absorption spectrum generated by a metal-to-ligand charge transfer (MLCT) electronic excited state, for instance, can be approximated using steady-state spectra generated by electrochemical ligand reduction and metal oxidation and accounting for loss of absorptions by the electronic ground state. However, the reliability of this approach can be clouded when multiple electronic configurations have similar optical signatures. Using a case study of Fe(II) complexes supported by benzannulated diarylamido ligands, we highlight an example of such an ambiguity and show how time-resolved X-ray emission spectroscopy (XES) measurements can reliably assign excited states from the perspective of the metal, particularly in conjunction with accurate synthetic models of ligand-field electronic excited states, leading to a re-interpretation of the long-lived excited state as a ligand-field metal-centered quintet state. A detailed analysis of the XES data on the long-lived excited state is presented, along with a discussion of the ultrafast dynamics following the photoexcitation of low-spin Fe(II)-N_{amido} complexes using a high-spin ground-state analogue as a spectral model for the $^5T_2$ excited state.

INTRODUCTION

For discrete, homogeneous molecules, light-driven reactivity including photocatalysis,[1,2] photodynamic therapy,[3] and wide bandgap semi-conductor photosensitization,[4] is generally more facile when mediated by long-lived charge-separated excited states. In such excited electronic configurations, spatial separation of charges helps sustain the chemical potential needed to drive photo-induced electron transfer.[5] For transition metal coordination complexes which can strongly absorb visible light, this typically takes the form of metal-to-ligand or ligand-to-metal charge-transfer character (MLCT/LMCT) excitation.[6] Chromophores comprised of 4d and 5d transition metals — for example, ruthenium(II) tris(2,2'-bipyridine) $[Ru(bpy)_3]^{2+}$ or iridium(III) tris(2-phenylpyridine) ($Ir(ppy)_3$) — can have long-lived MLCT states, as the strong ligand fields of these heavier metals destabilize metal-centered excited states relative to MLCT ones.[7] However, the environmental consequences of resource extraction and limitations on wide-spread adoption due to the low abundance of such elements[8] has spurred vigorous attempts to reproduce the profitable light-harvesting properties of $[Ru(bpy)_3]^{2+}$ or $Ir(ppy)_3$ in complexes of more abundant materials with Fe at the forefront.[9]

Focusing on the privileged electronic structure and geometry of pseudo-octahedral d^6 complexes,[10] the major challenge is overcoming the weaker ligand fields intrinsic to 3d metals that facilitate rapid deactivation of MLCT excited states through energetically accessible metal centered (MC) ones.[11] Ligand design has led to exciting, but still limited, successes for both ferrous complexes[12–15] and isoelectronic first-row metals.[16] A key tool in all these studies has been the assignment of CT character to excited states through their optical absorption profiles, typically observed using UV-Vis pump-probe transient absorption (TA) spectroscopy (Figure 1a).[17] The presence/absence of excited state absorption (ESA) features and bleaches of ground-state

absorptions in the TA spectra are compared with optical signatures of oxidized metal cores and reduced ligand arms gleaned from electrochemically generated absorption spectra to identify charge-transfer (e.g., MLCT) character.[18]

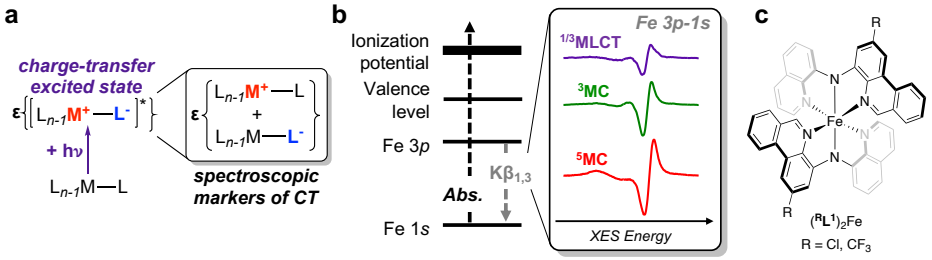

Figure 1. Schematic of (a) TA/spectroelectrochemistry approach and (b) the trXES experiment and examples of diagnostic spectra for excited state assignment in transition metal coordination complexes such as the highly covalent Fe-amido complexes shown in (c).

While this approach is valuable, it also has important limitations: the oxidized and reduced complexes may not always be stable on the timescale of the spectroelectrochemistry experiments, or the spectral signals provided by the reduced and oxidized complexes might not be sufficiently distinct from metal-centered excited states that are often involved in the relaxation of the CT excited states. Thus, the logical simplicity of this approach can belie the complexity in excited state properties[19] and prevent a true (or reliable) delineation of the dynamics involved. Time-resolved iron Kβ X-ray emission spectroscopy (trXES), on the other hand, allows for the ultrafast dynamics of a coordination complex's excited states to be probed directly from the perspective of the metal.[20–27] As the Kβ main line fluorescence signal is predominantly sensitive to the 3d spin moment, the technique can enable a more robust differentiation of the character of excited states

which may be involved in a decay cascade (Figure 1b).[28] Here, we demonstrate how trXES in conjunction with high-spin synthetic models can overcome ambiguities in excited state assignments via the optical TA/spectroelectrochemistry approach and conclusively reassign the optically active long-lived excited state in a series of highly covalent Fe-amido complexes, $(^{R}\mathbf{L}^{1})_2$Fe (Figure 1c).[29,30]

RESULTS AND DISCUSSION

Panchromatic absorbing pseudo-octahedral Fe(II) complexes ($^{R}\mathbf{L}^{1}$)$_2$Fe supported by (2-*R*-4-phenanthridinyl-8-quinolinyl)amido ligands (R = CF_3, *t*Bu or Cl) exhibit long-lived excited states with a strong, well-resolved ESA in the visible region (~480 nm; Figure 2a).[29] This optical signature, in conjunction with a bleach of the ground state absorptions between ~500-800 nm, is faithfully reproduced by the difference spectrum generated by spectroelectrochemistry, supporting a CT assignment.[30] In these molecules, strong mixing between filled Fe d and N_{amido}(2p) orbitals proffers Fe-N_{amido} π-antibonding character to the highest occupied molecular orbitals, resulting in formal 'π-antibonding-to-ligand' charge-transfer (PALCT) character.[31] The use of weak-field π-donor amido ligands, however, defies conventional photosensitizer design principles which typically rely on increasingly strong σ-donating ligands to destabilize MC excited states and thereby decrease the rates of nonradiative decay through ligand field channels.[32] This prompted a closer look at what sort of difference spectrum might be expected should a high-spin metal-centered excited state instead dominate the excited state decay cascade.

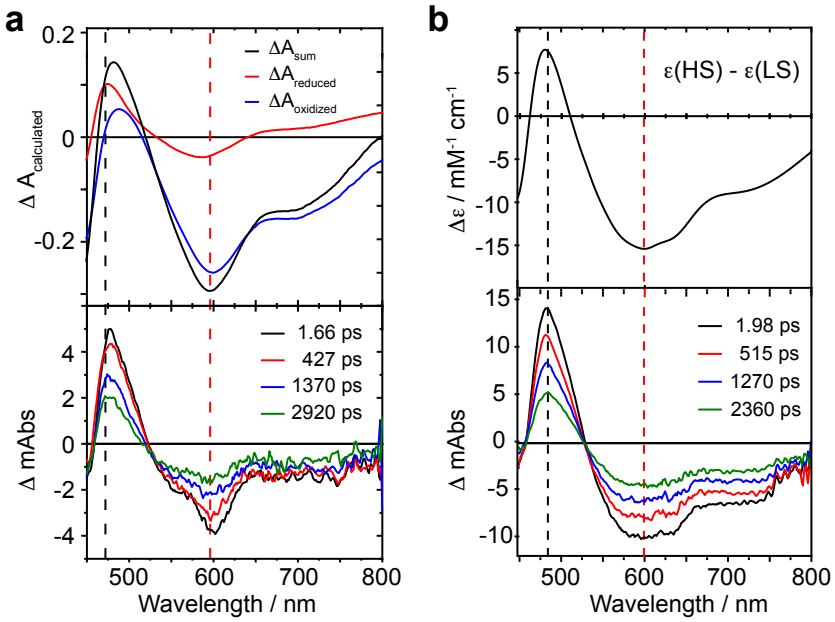

Figure 2. (a) Optical transient absorption spectra and spectroelectrochemically generated difference spectrum for $(^{Cl}\mathbf{L}^{1})_2$Fe;[30] (b) HS-LS difference spectrum for $(^{CF3}\mathbf{L}^{1})_2$Fe/$(^{CF3}\mathbf{L}^{2})_2$Fe overlaid with transient absorption spectra for $(^{CF3}\mathbf{L}^{1})_2$Fe adapted with permission from Springer Nature from reference[29]. Copyright 2019 Springer Nature.

Quintet MC states (such as the lowest energy quintet $^5T_2$ associated with octahedral complexes) have been found to form rapidly on decay of initially formed $^{1/3}$MLCT states through short-lived ^{3}MC states for many iron polypyridyls, including $[Fe(bpy)_3]^{2+}$.[22,33–36] To access a model of a photo-generated ^{5}MC for $(^{R}\mathbf{L}^{1})_2$Fe, we constructed a proligand with a methyl substituent on the 6-position of the phenanthridinyl donor arms ($^{CF3}\mathbf{L}^{2}$H) and used it to build a distorted Fe(II) complex $(^{CF3}\mathbf{L}^{2})_2$Fe (Figure 3a; see SI for full details). Previous studies demonstrated introducing

steric hindrance between two tridentate ligands effectively induces geometric distortions[37] that reduce metal-ligand overlap sufficiently so as to stabilize high-spin (HS) ground-states in Fe(II) *bis*(terpyridines).[38] The high-spin character of $(^{CF3}\mathbf{L}^{2})_2$Fe was confirmed as a quintet ground-state via a combination of single crystal XRD, SQUID magnetometry and ^{57}Fe Mössbauer spectroscopy[39–41] (Figure 3b-d), supported by broad, paramagnetically shifted NMR spectra. For example, when comparing the solid-state structure of $(^{CF3}\mathbf{L}^{2})_2$Fe to the previously reported low-spin (LS, $S = 0$) analogue $(^{CF3}\mathbf{L}^{1})_2$Fe,[29] all six Fe-N bonds are longer (Table S1) consistent with the targeted weaker metal-ligand overlap. The effective magnetic moment (5.12 μ_B), isomer shift {0.956(4) mm s^{-1}} and quadrupole splitting {1.77(1) mm s^{-1}} are each similarly consistent with high-spin $S = 2$ Fe(II).

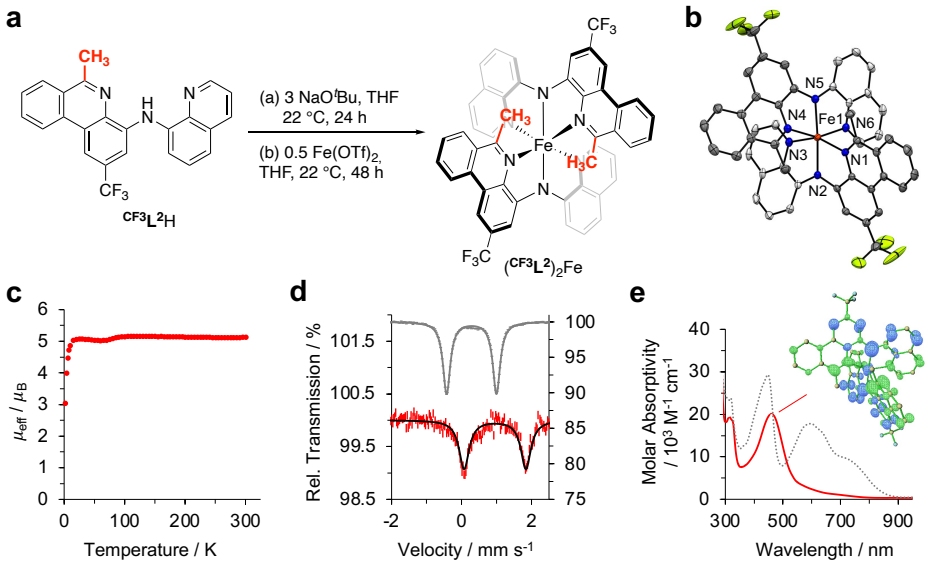

Figure 3. (a) Synthesis of the high-spin model of the $^5T_2$ excited state $(^{CF3}\mathbf{L}^{2})_2$Fe and its (b) solid-state X-ray crystal structure with thermal ellipsoids shown at 50% probability levels and hydrogen

atoms omitted for clarity, (c) magnetic susceptibility, (d) ^{57}Fe Mössbauer spectrum (150 K), and (e) ground-state absorption spectrum with the electron-hole map of the highest oscillator strength transition calculated to contribute to the low energy band overlaid (isosurface value = 0.002). In (d) and (e), the corresponding spectra for low-spin (^{CF3}**L**^{1})$_2$Fe are shown in grey.

Steady-state absorption spectra for (^{CF3}**L**^{2})$_2$Fe collected in acetonitrile contain intense absorption bands in the UV (owing to ligand-based transitions) and blue regions, with a λ_{max} of 461 nm (Figure 3e). The lowest energy absorption band is a result of mixed MLCT/ILCT (intra-ligand) transitions, exemplified by the electron-hole map shown as an inset in Figure 3e. In general, high-spin Fe(II) polypyridyls tend to be rather weakly absorbing in the visible range of the electromagnetic spectrum.[42–44] Thus, despite the weaker metal-ligand interactions induced by increased ligand sterics, the combination of π-donor amido ligands and benzannulated acceptor arms conspire to produce a rather unique absorption profile for (^{CF3}**L**^{2})$_2$Fe. Remarkably, the difference spectrum generated by subtracting the steady-state absorption spectrum of (^{CF3}**L**^{1})$_2$Fe from that of the high-spin ^{5}T$_2$ excited state model (^{CF3}**L**^{2})$_2$Fe also reconstructs the two main features of the TA spectra (Figure 2b). This indicates the ESA feature observed in the TA spectra of Fe(II)-N$_{amido}$ compounds could result from the ^{5}MC state absorbing in the same region. We therefore turned to trXES for a clearer assignment.

Time-Resolved and Steady State X-Ray Emission Spectroscopy (XES)

Given the distinctive electronic structures of Fe(II)-amido complexes compared to conventional Fe(II) polypyridyls, steady-state Fe Kβ main line XES spectra were collected for a low-spin complex {S = 0; (^{CF3}**L**^{1})$_2$Fe} and the high-spin model complex {S = 2; (^{CF3}**L**^{2})$_2$Fe} to better simulate the spectral features that might accompany formation of a ^{5}MC excited state. The difference of the S = 2 and S = 0 reference spectra was used as a spectral model for a quintet metal-centered excited state (Figure 4a). Picosecond (ps) time-resolved Fe Kβ main line XES spectra were then collected for (^{Cl}**L**^{1})$_2$Fe at a fixed pump-probe delay of 60 ps using a pump wavelength of 515 nm. The resulting difference spectrum is shown along with the constructed difference spectra for a ^{5}MC excited state (Figure 4a) and an MLCT excited state (Figure 4b). The MLCT excited state will be referred to herein as ^{2}PALCT (*vide infra*) from the perspective of the metal center, as the spin state of the metal center would be a doublet in this case. The difference spectrum for a ^{5}MC excited state was generated as described above, while the difference spectrum for the ^{2}PALCT excited state was constructed using reference spectra for S = ½ and S = 0 measured with the same XES spectrometer[45] at the SSRL and taken from Zhang *et al*.[22] Figure 4a shows that the experimentally obtained difference spectrum at 60 ps is in good agreement with the ^{5}MC constructed spectrum (R^2 = 0.9903), whereas it does not fit well with the ^{2}PALCT excited state model (R^2 = 0.8688; Figure 4b). The kinetic trace at the fixed emission energy of ~7056 eV could be fitted to a decay constant of τ = 3300 ± 300 ps (Figure 4c), which is in agreement with the lifetime of the long-lived excited state obtained from the optical TA measurements.[29] This strongly suggests the reported long-lived excited state for (^{R}**L**^{1})$_2$Fe complexes is ^{5}MC in nature.

Commented [DH1]: Marco, corrected based on your comment in SI page SI-12 that steady state was NOT collected for chloro compound…

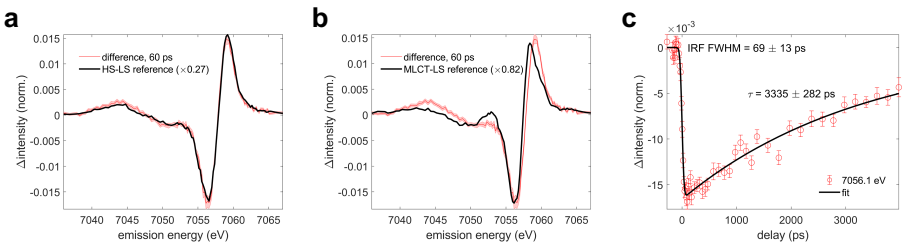

Figure 4. Fe Kβ main line X-ray emission spectroscopy of $(^{Cl}\mathbf{L}^{1})_2$Fe dissolved in toluene showing (a) the difference spectrum at 60 ps (red). Error bars represent the standard error of 25 individual area-normalized scans. The black line represents the scaled difference of Fe-amido HS ($S = 2$) and LS ($S = 0$) reference spectra; (b) a comparison of the difference spectrum from (a) with the scaled difference of independently measured MLCT ($S = 1/2$) and LS ($S = 0$) reference spectra taken from ref[22] (black); and (c) the time dependence of the difference signal at a fixed emission energy of ~7056 eV (red). The black line represents a mono-exponential decay multiplied by a Heaviside step function and convolved with a Gaussian instrument response function (IRF). Error bars of the kinetic trace represent the standard error of 26 scans.

Next, we looked at the valence-to-core (VtC) X-ray emission spectrum of $(^{Cl}\mathbf{L}^{1})_2$Fe. Experimental details can be found in the Supporting Information. Figure 5a shows the pumped and unpumped valence-to-core X-ray emission spectra. Notably, a significant shift of the emission energy upon the population of the long-lived excited state is not observed. Rather, a decrease is seen in VtC intensity, as expected for a ^{5}MC excited state because of the reduction of metal-ligand overlap due to lengthening of the metal-ligand bonds. The absence of an energy shift of the valence-to-core spectrum – expected for a CT excited state – further supports our assignment of the long-lived excited state character to a ^{5}MC excited state. Density Functional Theory (DFT) calculations were performed to simulate the valence-to-core X-ray emission spectra for the ground state and the ^{5}MC excited state using the ORCA 4.2.1 package.[46] The calculated spectra are shown in Figure 5b, where the calculated ^{5}MC spectrum reproduces the overall intensity reduction observed in the experimental pumped spectrum at 60 ps. The difference between the calculated

^{5}MC and ground state spectra was then compared with the experimental difference spectrum. Using a scaling factor of 0.27, consistent with the population of the ^{5}MC excited state extracted from the Kβ main line analysis, qualitative agreement between the calculated and experimental difference spectra could be obtained (Figure 5c). This reaffirms the conclusions derived from the analysis of the Fe Kβ main line XES: the excited state that persists for ns is a metal-centered quintet.

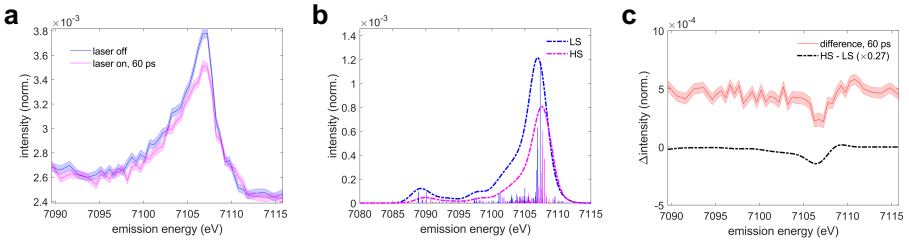

Figure 5. Valence-to-core X-ray emission spectroscopy of $(^{Cl}\mathbf{L}^1)_2$Fe dissolved in toluene showing (a) the measured unpumped spectrum (blue) and the pumped spectrum after a 60 ps time delay (magenta). Error bars represent the standard error of 194 individual area-normalized scans; (b) the calculated valence-to-core transitions for the LS (S = 0, blue) and HS (S = 2, magenta) configurations. A broadening of 3 eV has been applied; and (c) the experimental difference spectrum (laser on minus laser off) at a 60 ps time delay (red line) with the scaled difference of the calculated HS and LS spectra (black dashed line). The scaling factor for the calculated difference spectrum is taken from the fit of the Kβ main line difference spectrum shown in Figure 4a.

Spectrotemporal modeling of the femtosecond X-ray emission spectra

The ps resolution XES data presented in the previous section provides strong evidence that the long-lived excited state has metal-centered quintet character, but this does not address either the wavelength dependence of the relaxation mechanism nor the rate of ^{5}MC formation. To address these issues, we complemented the ps-resolution measurements from SSRL with femtosecond measurements of $(^{CF3}\mathbf{L}^1)_2$Fe at the LCLS using an optical pump centered at 800 nm. For ferrous

complexes, short-lived ^{3}MC excited states are often invoked as transient electronic configurations populated during the transition between photoexcited CT excited states and longer lived ^{5}MC states.[22,47] A singular value decomposition of the data in the entire delay range and subsequent data reconstruction suggests only two significant spectral components (Figure S3). Therefore, to determine whether the data provides robust evidence of any transient intermediate electronic excited state populated following the decay of the ^{2}PALCT excited state and before the formation of the ^{5}MC excited state, we considered different spectrotemporal models. We examined two pathways either with or without a detectable ^{3}MC intermediate. The experimental Kβ main line difference spectrum $\Delta I_{K\beta}$ was therefore fitted using the following fit equation:

$$\Delta I_{K\beta}(t_i,E_j) = \sum_k N_k\,(t_i) \cdot \Delta I_k(E_j)$$

The summation includes a combination of the ^{2}PALCT, ^{5}MC and the ^{3}MC excited states. The ^{2}PALCT excited state is modeled using a difference spectrum based on independently measured Fe(II) reference spectra with $S = ½$ and $S = 0$, taken from Zhang *et al*.[22] For the ^{5}MC excited state we utilized a difference spectrum constructed using the first spectral component of a singular value decomposition of the time-dependent Fe Kβ main line difference map limited to time delays after 0.5 ps, where spectral contributions of the short-lived intermediate species should be negligible (see SI for a short discussion on this choice). After determining the time-dependent populations N_k, they were then multiplied by a Heaviside function $H(t-t_0)$ and convoluted with a Gaussian instrument response function, where the excitation fraction f_{exc}, the excited state lifetimes τ_{PALCT}, τ_{3MC}, τ_{5MC}, and time zero t_0 were determined for each model via a least-squares fitting procedure. This procedure is detailed in the SI. The optimized values using the first SVD-component of the femtosecond XES data after 0.5 ps as a model for the ^{5}MC excited state difference spectrum are shown in Table 1 for the two different models. Fits and time dependent populations are shown in

Figures 6 and S4. Table 1 also presents RSS-values and small-sample corrected Akaike weights w_i.[48,49] These values indicate that only statistically insignificant improvements in the fit were achieved using the more complex model with a ^{3}MC intermediate via ^{2}PALCT $\rightarrow$ ^{3}MC $\rightarrow$ ^{5}MC; the ^{2}PALCT $\rightarrow$ ^{5}MC model was sufficient to represent the experiment. For both models, the photo-excitation fraction f_{exc} was fitted to ~0.55 and the ^{2}PALCT excited state decayed within ~150 fs. An F-test of the two models with different number of parameters p_1 and p_2 (Table S2) confirms the conclusions from Table 1. These findings should not be interpreted to confirm ^{3}MC states do not participate in the spin crossover mechanism for $(^{\mathbf{CF3}}\mathbf{L}^{\mathbf{1}})_2$Fe. Alternatively, τ_{PALCT} could far exceed τ_{3MC} making the ^{3}MC unobservable but still mechanistically significant. This would depend on the strength of the spin-orbit coupling between CT and MC excited states, and prior theoretical calculations have predicted weak interactions between ^{3}MLCT and ^{5}MC excited states for polypyridyl Fe complexes.[50,51] Whether the greater covalency of the Fe(II) benzannulated diarylamido complexes[30] significantly modifies the strength of the spin-orbit coupling requires further investigation.

Table 1. Summary of the fits using the spectrotemporal models (A: $^2PALCT \rightarrow {}^5MC$, B: $^2PALCT \rightarrow {}^3MC \rightarrow {}^5MC$) described in the text. RSS values are multiplied by 1000. RSS values in brackets are evaluated in limited temporal and spectral ranges (7040 – 7070 eV, -0.1 –0.5 ps) while the fit is maintained on the full range. The respective Akaike weights are indicated in brackets.

Model	f_{exc} / -	τ_{PALCT} / fs	τ_{3MC} / fs	τ_{5MC} / ps	σ_{IRF} / fs	t_0 / fs	RSS / a.u.	w_i / -	R^2 / -
A	0.55	122	-	3329	62	58	9.9769 (3.4626)	0.75 (0.73)	0.99
B	0.55	113	21	3329	62	56	9.9570 (3.442)	0.25 (0.27)	0.99

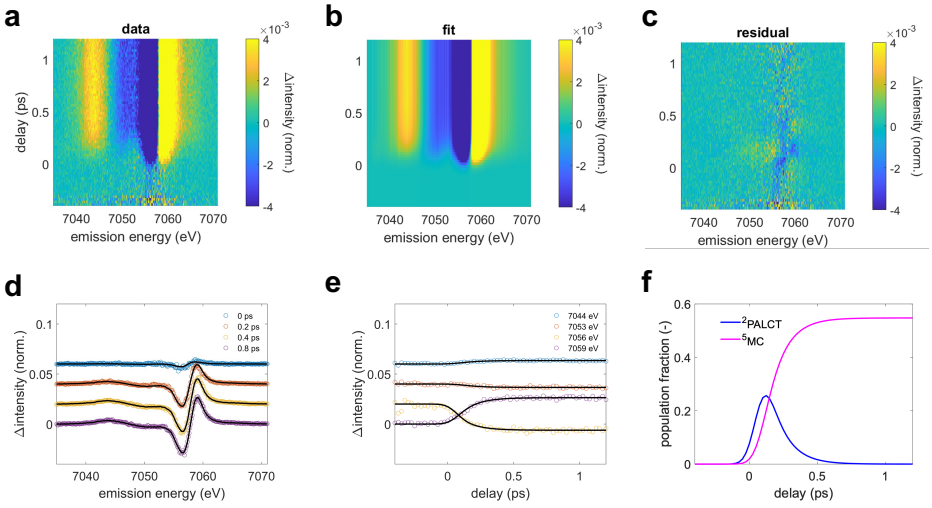

Figure 6. Fit of the time dependent Fe Kβ main line difference spectra using a spectrotemporal model including ^{2}PALCT and ^{5}MC excited states, including (a-c) the time dependent difference spectra together with the spectrotemporal model fit and the residual; (d) difference spectra at different time delays with the fits (black lines); (e) kinetic traces at different emission energies together with the fits (black lines); and (f) the time dependent populations.

CONCLUSIONS

Ultrafast trXES measurements have clarified the ambiguous interpretation from ultrafast optical spectroscopy of low-spin Fe(II)-N_{amido} complexes ($^{R}\mathbf{L}^{1}$)$_2$Fe,[29] demonstrating unequivocally the long-lived electronic excited state for these low-spin systems has a metal-centered quintet spin state configuration with the same lifetime as the long-lived excited state observed with optical pump-probe spectroscopy. Femtosecond XES measurements revealed optically initiated spin crossover occurs with a ~150 fs time constant, similar to other Fe complexes.[22,33–36,47] These measurements did not robustly observe the initially generated CT excited state due to the time resolution of the measurement and the comparatively weak CT difference signal when probed with XES. The qualitative potential energy surfaces extrapolated from DFT calculations would indicate a ^{3}MC intermediate should be formed during optically driven spin crossover, but the kinetic modeling does not show a detectable population build-up of such an intermediate.

The similar relaxation dynamics with respect to other Fe polypyridyl complexes and high quantum yield for ^{5}MC formation indicates that the strong covalency of the Fe amido bond is not sufficient to significantly change the potential energy surfaces that control the lifetimes of these Fe complexes. RIXS measurements confirmed the viability of using metal-ligand covalency to destabilize metal-centered excited states relative to the CT excited states at the ground-state geometry,[30] but the measurements presented here demonstrate the effect is insufficient for these specific Fe amido complexes to significantly extend the CT excited state lifetime. Our study shows the need to proceed with caution when using spectroelectrochemistry to interpret ultrafast optical pump-probe spectroscopic measurements and highlights the valuable insight that can be provided by ultrafast XES and high-spin model complexes. The gradual emergence of dedicated ultrafast

XES end-stations[25,52–55] is expanding the possibilities for the ultrafast research community to systematically incorporate these advanced characterization tools into their arsenal.

ASSOCIATED CONTENT

Supporting Information. Full details regarding instrumentation and methods; synthetic methodology, multi-nuclear NMR and HR-MS spectra for all compounds; description of computational methodology, data tables, figures, and coordinates; additional XES figures, tables and discussion. CCDC 2307656 contains the supplementary crystallographic data for this paper which can be obtained free of charge from the Cambridge Crystallographic Data Center via www.ccdc.cam.ac.uk/structures.

The following files are available free of charge:

Supporting Information File (PDF)

Crystallographic Information Files (CIF)

AUTHOR INFORMATION

Corresponding Authors

David E. Herbert (david.herbert@umanitoba.ca)

Dimosthenis Sokaras (dsokaras@slac.stanford.edu)

Kelly J. Gaffney (kgaffney@slac.stanford.edu)

ORCIDs

Marco E. Reinhard: 0000-0001-7155-2011

Baldeep K. Sidhu: 0000-0002-2016-6601

Issiah B. Lozada: 0000-0002-1689-2918

Robert J. Ortiz: 0000-0001-9078-765X

Hyeongtaek Lim: 0000-0003-3470-8296

Natalia Powers-Riggs: 0000-0002-9309-9622

Rachel Nickel: 0000-0002-8179-6295

Johan van Lierop: 0000-0001-9398-4835

Amy A. Cordones: 0000-0001-9897-5380

Dimosthenis Sokaras: 0000-0001-8117-1933

Kelly J. Gaffney: 0000-0002-0525-6465

David E. Herbert: 0000-0001-8190-2468

Author Contributions

All authors have given approval to the final version of the manuscript.

Conflicts of Interest

There are no conflicts of interest to declare.

ACKNOWLEDGMENTS

NPR, HL, SLR, AAC and KJG thank the U.S. Department of Energy, Office of Science, Office of Basic Energy Sciences, Chemical Sciences, Geosciences and Biosciences Division for supporting this work. Further support for this work came from the Natural Sciences Engineering Research Council of Canada for RGPIN-2022-04501 (DEH), RGPIN-2018-05012 (JvL) and CGS-D Fellowships to BKS and RJO. Use of the Linac Coherent Light Source (LCLS), SLAC National Accelerator Laboratory, was supported by the U.S. Department of Energy, Office of Science, Office of Basic Energy Sciences under Contract No. DE-AC02-76SF00515. The Stanford Synchrotron Radiation Lightsource, SLAC National Accelerator Laboratory, was supported by the

U.S. Department of Energy, Office of Science, Office of Basic Energy Sciences under Contract No. DE-AC02–76SF00515. DFT calculations were supported with resources from the SSRL Structural Molecular Biology Program supported by the DOE Office of Biological and Environmental Research, and by the National Institutes of Health, National Institute of General Medical Sciences (No. P30GM133894) and Compute Canada. This research used resources of the National Energy Research Scientific Computing Center (NERSC), a U.S. Department of Energy Office of Science User Facility operated under Contract No. DE-AC02-05CH11231.

References

(1) Prier, C. K.; Rankic, D. A.; MacMillan, D. W. C. Visible Light Photoredox Catalysis with Transition Metal Complexes: Applications in Organic Synthesis. *Chem. Rev.* **2013**, *113*, 5322−5363.
(2) Dalle, K. E.; Warnan, J.; Leung, J. J.; Reuillard, B.; Karmel, I. S.; Reisner, E. Electro- and Solar-Driven Fuel Synthesis with First Row Transition Metal Complexes. *Chem. Rev.* **2019**, *119*, 2752–2875.
(3) Gourdon, L.; Cariou, K.; Gasser, G. Phototherapeutic Anticancer Strategies with First-Row Transition Metal Complexes: A Critical Review. *Chem. Soc. Rev.* **2022**, *51*, 1167–1195.
(4) Behm, K.; McIntosh, R. D. Application of Discrete First-Row Transition-Metal Complexes as Photosensitisers. *ChemPlusChem* **2020**, *85*, 2611–2618.
(5) Arias-Rotondo, D. M.; McCusker, J. K. The Photophysics of Photoredox Catalysis: A Roadmap for Catalyst Design. *Chem. Soc. Rev.* **2016**, *45*, 5803–5820.
(6) Förster, C.; Heinze, K. Bimolecular Reactivity of 3d Metal-Centered Excited States (Cr, Mn, Fe, Co). *Chem. Phys. Rev.* **2022**, *3*, 041302.
(7) Wenger, O. S. Is Iron the New Ruthenium? *Chem. - Eur. J.* **2019**, *25*, 6043–6052.
(8) Graedel, T. E.; Harper, E. M.; Nassar, N. T.; Nuss, P.; Reck, B. K. Criticality of Metals and Metalloids. *Proc. Nat. Acad. Sci.* **2015**, *112*, 4257–4262.
(9) Wenger, O. S. Photoactive Complexes with Earth-Abundant Metals. *J. Am. Chem. Soc.* **2018**, *140*, 13522–13533.
(10) Sinha, N.; Wenger, O. S. Photoactive Metal-to-Ligand Charge Transfer Excited States in 3d6 Complexes with Cr0, MnI, FeII, and CoIII. *J. Am. Chem. Soc.* **2023**, *145*, 4903–4920.
(11) McCusker, J. K. Electronic Structure in the Transition Metal Block and Its Implications for Light Harvesting. *Science* **2019**, *363*, 484.
(12) Liu, Y.; Warnmark, K.; Liu, Y.; Sundstrom, V.; Persson, P. Fe N-Heterocyclic Carbene Complexes as Promising Photosensitizers. *Acc. Chem. Res.* **2016**, *49*, 1477–1485.
(13) Reuter, T.; Kruse, A.; Schoch, R.; Lochbrunner, S.; Bauer, M.; Heinze, K. Higher MLCT Lifetime of Carbene Iron(II) Complexes by Chelate Ring Expansion. *Chem. Commun.* **2021**, *57*, 7541–7544.
(14) Leis, W.; Argüello Cordero, M. A.; Lochbrunner, S.; Schubert, H.; Berkefeld, A. A Photoreactive Iron(II) Complex Luminophore. *J. Am. Chem. Soc.* **2022**, *144*, 1169–1173.
(15) Malme, J. T.; Clendening, R. A.; Ash, R.; Curry, T.; Ren, T.; Vura-Weis, J. Nanosecond Metal-to-Ligand Charge-Transfer State in an Fe(II) Chromophore: Lifetime Enhancement via Nested Potentials. *J. Am. Chem. Soc.* **2023**, *145*, 6029–6034.
(16) Sinha, N.; Wegeberg, C.; Häussinger, D.; Prescimone, A.; Wenger, O. S. Photoredox-Active Cr(0) Luminophores Featuring Photophysical Properties Competitive with Ru(II) and Os(II) Complexes. *Nat. Chem.* **2023**, *15*, 1730–1736.
(17) Cebrián, C.; Pastore, M.; Monari, A.; Assfeld, X.; Gros, P. C.; Haacke, S. Ultrafast Spectroscopy of Fe(II) Complexes Designed for Solar-Energy Conversion: Current Status and Open Questions. *ChemPhysChem* **2022**, *23*, e202100659.
(18) Brown, A. M.; McCusker, C. E.; McCusker, J. K. Spectroelectrochemical Identification of Charge-Transfer Excited States in Transition Metal-Based Polypyridyl Complexes. *Dalton Trans.* **2014**, *43*, 17635–17646.

(19) Lindh, L.; Pascher, T.; Persson, S.; Goriya, Y.; Wärnmark, K.; Uhlig, J.; Chábera, P.; Persson, P.; Yartsev, A. Multifaceted Deactivation Dynamics of Fe(II) N-Heterocyclic Carbene Photosensitizers. *J. Phys. Chem. A* **2023**, *127*, 10210–10222.
(20) Vankó, G.; Glatzel, P.; Pham, V.-T.; Abela, R.; Grolimund, D.; Borca, C. N.; Johnson, S. L.; Milne, C. J.; Bressler, C. Picosecond Time-Resolved X-Ray Emission Spectroscopy: Ultrafast Spin-State Determination in an Iron Complex. *Angew. Chem., Int. Ed.* **2010**, *49*, 5910.
(21) Vankó, G.; Bordage, A.; Glatzel, P.; Gallo, E.; Rovezzi, M.; Gawelda, W.; Galler, A.; Bressler, C.; Doumy, G.; March, A. M.; Kanter, E. P.; Young, L.; Southworth, S. H.; Canton, S. E.; Uhlig, J.; Smolentsev, G.; Sundström, V.; Haldrup, K.; van Driel, T. B.; Nielsen, M. M.; Kjaer, K. S.; Lemke, H. T. Spin-State Studies with XES and RIXS: From Static to Ultrafast. *J. Electron Spectrosc. Relat. Phenom.* **2013**, *188*, 166–171.
(22) Zhang, W.; Alonso-Mori, R.; Bergmann, U.; Bressler, C.; Chollet, M.; Galler, A.; Gawelda, W.; Hadt, R. G.; Hartsock, R. W.; Kroll, T.; Kjær, K. S.; Kubiček, K.; Lemke, H. T.; Liang, H. W.; Meyer, D. A.; Nielsen, M. M.; Purser, C.; Robinson, J. S.; Solomon, E. I.; Sun, Z.; Sokaras, D.; van Driel, T. B.; Vankó, G.; Weng, T.-C.; Zhu, D.; Gaffney, K. J. Tracking Excited-State Charge and Spin Dynamics in Iron Coordination Complexes. *Nature* **2014**, *509*, 345–348.
(23) Miaja-Avila, L.; O'Neil, G. C.; Joe, Y. I.; Alpert, B. K.; Damrauer, N. H.; Doriese, W. B.; Fatur, S. M.; Fowler, J. W.; Hilton, G. C.; Jimenez, R.; Reintsema, C. D.; Schmidt, D. R.; Silverman, K. L.; Swetz, D. S.; Tatsuno, H.; Ullom, J. N. Ultrafast Time-Resolved Hard X-Ray Emission Spectroscopy on a Tabletop. *Phys. Rev. X* **2016**, *6*, 031047.
(24) Gaffney, K. J. Capturing Photochemical and Photophysical Transformations in Iron Complexes with Ultrafast X-Ray Spectroscopy and Scattering. *Chem. Sci.* **2021**, *12*, 8010–8025.
(25) Reinhard, M.; Skoien, D.; Spies, J. A.; Garcia-Esparza, A. T.; Matson, B. D.; Corbett, J.; Tian, K.; Safranek, J.; Granados, E.; Strader, M.; Gaffney, K. J.; Alonso-Mori, R.; Kroll, T.; Sokaras, D. Solution Phase High Repetition Rate Laser Pump X-Ray Probe Picosecond Hard x-Ray Spectroscopy at the Stanford Synchrotron Radiation Lightsource. *Struct. Dyn.* **2023**, *10*, 054304.
(26) Reinhard, M.; Gallo, A.; Guo, M.; Garcia-Esparza, A. T.; Biasin, E.; Qureshi, M.; Britz, A.; Ledbetter, K.; Kunnus, K.; Weninger, C.; van Driel, T.; Robinson, J.; Glownia, J. M.; Gaffney, K. J.; Kroll, T.; Weng, T.-C.; Alonso-Mori, R.; Sokaras, D. Ferricyanide Photo-Aquation Pathway Revealed by Combined Femtosecond Kβ Main Line and Valence-to-Core x-Ray Emission Spectroscopy. *Nat. Commun.* **2023**, *14*, 2443.
(27) Guo, M.; Braun, A.; Sokaras, D.; Kroll, T. Iron Kβ X-Ray Emission Spectroscopy: The Origin of Spectral Features from Atomic to Molecular Systems Using Multi-Configurational Calculations. *J. Phys. Chem. A* **2024**, *128*, 1260–1273.
(28) Britz, A.; Gawelda, W.; Assefa, T. A.; Jamula, L. L.; Yarranton, J. T.; Galler, A.; Khakhulin, D.; Diez, M.; Harder, M.; Doumy, G.; March, A. M.; Bajnóczi, É.; Németh, Z.; Pápai, M.; Rozsályi, E.; Sárosiné Szemes, D.; Cho, H.; Mukherjee, S.; Liu, C.; Kim, T. K.; Schoenlein, R. W.; Southworth, S. H.; Young, L.; Jakubikova, E.; Huse, N.; Vankó, G.; Bressler, C.; McCusker, J. K. Using Ultrafast X-Ray Spectroscopy To Address Questions in Ligand-Field Theory: The Excited State Spin and Structure of $[Fe(Dcpp)_2]^{2+}$. *Inorg. Chem.* **2019**, *58*, 9341–9350.

(29) Braun, J. D.; Lozada, I. B.; Kolodziej, C.; Burda, C.; Newman, K. M. E.; van Lierop, J.; Davis, R. L.; Herbert, D. E. Iron(II) Coordination Complexes with Panchromatic Absorption and Nanosecond Charge-Transfer Excited State Lifetimes. *Nat. Chem.* **2019**, *11*, 1144–1150.
(30) Larsen, C. B.; Braun, J. D.; Lozada, I. B.; Kunnus, K.; Biasin, E.; Kolodziej, C.; Burda, C.; Cordones, A. A.; Gaffney, K. J.; Herbert, D. E. Reduction of Electron Repulsion in Highly Covalent Fe-Amido Complexes Counteracts the Impact of a Weak Ligand Field on Excited-State Ordering. *J. Am. Chem. Soc.* **2021**, *143*, 20645–20656.
(31) Braun, J. D.; Lozada, I. B.; Herbert, D. E. In Pursuit of Panchromatic Absorption in Metal Coordination Complexes: Experimental Delineation of the HOMO Inversion Model Using Pseudo-Octahedral Complexes of Diarylamido Ligands. *Inorg. Chem.* **2020**, *59*, 17746–17757.
(32) Förster, C.; Heinze, K. Photophysics and Photochemistry with Earth-Abundant Metals – Fundamentals and Concepts. *Chem. Soc. Rev.* **2020**, *49*, 1057–1070.
(33) Kjær, K. S.; Driel, T. B. V.; Harlang, T. C. B.; Kunnus, K.; Biasin, E.; Ledbetter, K.; Hartsock, R. W.; Reinhard, M. E.; Koroidov, S.; Li, L.; Laursen, M. G.; Hansen, F. B.; Vester, P.; Christensen, M.; Haldrup, K.; Nielsen, M. M.; Dohn, A. O.; Pápai, M. I.; Møller, K. B.; Chabera, P.; Liu, Y.; Tatsuno, H.; Timm, C.; Jarenmark, M.; Uhlig, J.; Sundstöm, V.; Wärnmark, K.; Persson, P.; Németh, Z.; Szemes, D. S.; Bajnóczi, É.; Vankó, G.; Alonso-Mori, R.; Glownia, J. M.; Nelson, S.; Sikorski, M.; Sokaras, D.; Canton, S. E.; Lemke, H. T.; Gaffney, K. J. Finding Intersections between Electronic Excited State Potential Energy Surfaces with Simultaneous Ultrafast X-Ray Scattering and Spectroscopy. *Chem. Sci.* **2019**, *10*, 5749–5760.
(34) Auböck, G.; Chergui, M. Sub-50-Fs Photoinduced Spin Crossover in [Fe(Bpy)3]2+. *Nature Chem* **2015**, *7*, 629–633.
(35) Cannizzo, A.; Milne, C. J.; Consani, C.; Gawelda, W.; Bressler, Ch.; van Mourik, F.; Chergui, M. Light-Induced Spin Crossover in Fe(II)-Based Complexes: The Full Photocycle Unraveled by Ultrafast Optical and X-Ray Spectroscopies. *Coord. Chem. Rev.* **2010**, *254*, 2677–2686.
(36) Bressler, Ch.; Milne, C.; Pham, V.-T.; ElNahhas, A.; van der Veen, R. M.; Gawelda, W.; Johnson, S.; Beaud, P.; Grolimund, D.; Kaiser, M.; Borca, C. N.; Ingold, G.; Abela, R.; Chergui, M. Femtosecond XANES Study of the Light-Induced Spin Crossover Dynamics in an Iron(II) Complex. *Science* **2009**, *323*, 489–492.
(37) Vallett, P. J.; Damrauer, N. H. Experimental and Computational Exploration of Ground and Excited State Properties of Highly Strained Ruthenium Terpyridine Complexes. *J. Phys. Chem. A* **2013**, *117*, 6489–6507.
(38) Shepard, S. G.; Fatur, S. M.; Rappé, A. K.; Damrauer, N. H. Highly Strained Iron(II) Polypyridines: Exploiting the Quintet Manifold To Extend the Lifetime of MLCT Excited States. *J. Am. Chem. Soc.* **2016**, *138*, 2949–2952.
(39) Constable, E. C.; Baum, G.; Bill, E.; Dyson, R.; van Eldik, R.; Fenske, D.; Kaderli, S.; Morris, D.; Neubrand, A.; Neuburger, M.; Smith, D. R.; Wieghardt, K.; Zehnder, M.; Zuberbühler, A. D. Control of Iron(II) Spin States in 2,2′:6′,2″-Terpyridine Complexes through Ligand Substitution. *Chem. Eur. J.* **1999**, *5*, 498–508.
(40) Suhr, S.; Schröter, N.; Kleoff, M.; Neuman, N.; Hunger, D.; Walter, R.; Lücke, C.; Stein, F.; Demeshko, S.; Liu, H.; Reissig, H.-U.; van Slageren, J.; Sarkar, B. Spin State in Homoleptic Iron(II) Terpyridine Complexes Influences Mixed Valency and Electrocatalytic CO2 Reduction. *Inorg. Chem.* **2023**, *62*, 6375–6386.

(41) Milocco, F.; de Vries, F.; Siebe, H. S.; Engbers, S.; Demeshko, S.; Meyer, F.; Otten, E. Widening the Window of Spin-Crossover Temperatures in Bis(Formazanate)Iron(II) Complexes via Steric and Noncovalent Interactions. *Inorg. Chem.* **2021**, *60*, 2045–2055.
(42) Constable, E. C.; Baum, G.; Bill, E.; Dyson, R.; van Eldik, R.; Fenske, D.; Kaderli, S.; Morris, D.; Neubrand, A.; Neuburger, M.; Smith, D. R.; Wieghardt, K.; Zehnder, M.; Zuberbühler, A. D. Control of Iron(II) Spin States in 2,2′:6′,2″-Terpyridine Complexes through Ligand Substitution. *Chem. Eur. J.* **1999**, *5*, 498–508.
(43) Fatur, S. M.; Shepard, S. G.; Higgins, R. F.; Shores, M. P.; Damrauer, N. H. A Synthetically Tunable System To Control MLCT Excited-State Lifetimes and Spin States in Iron(II) Polypyridines. *J. Am. Chem. Soc.* **2017**, *139*, 4493–4505.
(44) Moll, J.; Förster, C.; König, A.; Carrella, L. M.; Wagner, M.; Panthöfer, M.; Möller, A.; Rentschler, E.; Heinze, K. Panchromatic Absorption and Oxidation of an Iron(II) Spin Crossover Complex. *Inorg. Chem.* **2022**, *61*, 1659–1671.
(45) Sokaras, D.; Weng, T.-C.; Nordlund, D.; Velikov, P.; Wenger, D.; Garachtchenko, A.; George, M.; Borzenets, V.; Johnson, B.; Rabedeau, T.; Alonso-Mori, R.; Bergmann, U. A Seven-Crystal Johann-Type Hard x-Ray Spectrometer at the Stanford Synchrotron Radiation Lightsource. *Rev. Sci. Instrum.* **2013**, *84*.
(46) Neese, F. Software Update: The ORCA Program System, Version 4.0. *WIREs Computational Molecular Science* **2018**, *8*, e1327.
(47) Zhang, K.; Ash, R.; Girolami, G. S.; Vura-Weis, J. Tracking the Metal-Centered Triplet in Photoinduced Spin Crossover of Fe(Phen)32+ with Tabletop Femtosecond M-Edge X-Ray Absorption Near-Edge Structure Spectroscopy. *J. Am. Chem. Soc.* **2019**, *141*, 17180–17188.
(48) Burnham, K. P.; Anderson, D. R. *Model Selection and Inference. A Practical Information-Theoretic Approach.*; Springer: New York, NY, 1998.
(49) Reinhard, M. E.; Mara, M. W.; Kroll, T.; Lim, H.; Hadt, R. G.; Alonso-Mori, R.; Chollet, M.; Glownia, J. M.; Nelson, S.; Sokaras, D.; Kunnus, K.; Driel, T. B. van; Hartsock, R. W.; Kjaer, K. S.; Weninger, C.; Biasin, E.; Gee, L. B.; Hodgson, K. O.; Hedman, B.; Bergmann, U.; Solomon, E. I.; Gaffney, K. J. Short-Lived Metal-Centered Excited State Initiates Iron-Methionine Photodissociation in Ferrous Cytochrome c. *Nat. Commun.* **2021**, *12*, 1086.
(50) Sousa, C.; de Graaf, C.; Rudavskyi, A.; Broer, R.; Tatchen, J.; Etinski, M.; Marian, C. M. Ultrafast Deactivation Mechanism of the Excited Singlet in the Light-Induced Spin Crossover of [Fe(2,2′-Bipyridine)3]2+. *Chem. Eur. J.* **2013**, *19*, 17541–17551.
(51) Penfold, T. J.; Gindensperger, E.; Daniel, C.; Marian, C. M. Spin-Vibronic Mechanism for Intersystem Crossing. *Chem. Rev.* **2018**, *118*, 6975–7025.
(52) Alonso-Mori, R.; Kern, J.; Gildea, R. J.; Sokaras, D.; Weng, T.-C.; Lassalle-Kaiser, B.; Tran, R.; Hattne, J.; Laksmono, H.; Hellmich, J.; Glöckner, C.; Echols, N.; Sierra, R. G.; Schafer, D. W.; Sellberg, J.; Kenney, C.; Herbst, R.; Pines, J.; Hart, P.; Herrmann, S.; Grosse-Kunstleve, R. W.; Latimer, M. J.; Fry, A. R.; Messerschmidt, M. M.; Miahnahri, A.; Seibert, M. M.; Zwart, P. H.; White, W. E.; Adams, P. D.; Bogan, M. J.; Boutet, S.; Williams, G. J.; Zouni, A.; Messinger, J.; Glatzel, P.; Sauter, N. K.; Yachandra, V. K.; Yano, J.; Bergmann, U. Energy-Dispersive X-Ray Emission Spectroscopy Using an X-Ray Free-Electron Laser in a Shot-by-Shot Mode. *Proc. Natl. Acad. Sci.* **2012**, *109*, 19103–19107.
(53) March, A. M.; Assefa, T. A.; Boemer, C.; Bressler, C.; Britz, A.; Diez, M.; Doumy, G.; Galler, A.; Harder, M.; Khakhulin, D.; Németh, Z.; Pápai, M.; Schulz, S.; Southworth, S. H.; Yavaş, H.; Young, L.; Gawelda, W.; Vankó, G. Probing Transient Valence Orbital Changes

with Picosecond Valence-to-Core X-Ray Emission Spectroscopy. *J. Phys. Chem. C* **2017**, *121*, 2620–2626.
(54) Khakhulin, D.; Otte, F.; Biednov, M.; Bömer, C.; Choi, T.-K.; Diez, M.; Galler, A.; Jiang, Y.; Kubicek, K.; Lima, F. A.; Rodriguez-Fernandez, A.; Zalden, P.; Gawelda, W.; Bressler, C. Ultrafast X-Ray Photochemistry at European XFEL: Capabilities of the Femtosecond X-Ray Experiments (FXE) Instrument. *Appl. Sci.* **2020**, *10*, 995.
(55) Bacellar, C.; Kinschel, D.; Mancini, G. F.; Ingle, R. A.; Rouxel, J.; Cannelli, O.; Cirelli, C.; Knopp, G.; Szlachetko, J.; Lima, F. A.; Menzi, S.; Pamfilidis, G.; Kubicek, K.; Khakhulin, D.; Gawelda, W.; Rodriguez-Fernandez, A.; Biednov, M.; Bressler, C.; Arrell, C. A.; Johnson, P. J. M.; Milne, C. J.; Chergui, M. Spin Cascade and Doming in Ferric Hemes: Femtosecond X-Ray Absorption and X-Ray Emission Studies. *Proc. Natl. Acad. Sci.* **2020**, *117*, 21914–21920.

TOC Graphic

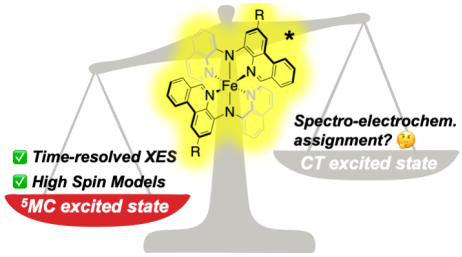
R
*
N
N
N
Fe
N
N
R
Spectro-electrochem.
assignment?
CT excited state
Time-resolved XES
High Spin Models
5MC excited state